Materials Research, Vol. 4, No. 3, 217-222, 2001.

Wet Processing and Characterization of ZrO_2/Stainless Steel Composites: Electrical and Mechanical Perfomance

S. López-Esteban[a], *J.F. Bartolomé*[a], *C. Pecharromán*[a], *S.R.H. Mello Castanho*[b*], *J.S. Moya*[a]

[a] *Instituto de Ciencia de Materiales de Madrid (ICMM), CSIC, Cantoblanco, 28049 Madrid, Spain*
[b] *Instituto de Pesquisas Energéticas e Nucleares, Trav. R, n. 400, USP, 05508-900 São Paulo - SP, Brasil*

Received: February 1, 2001; Revised: June 5, 2001

Zirconia/stainless steel composites have been prepared by a wet processing method with metal volume concentration ranging from 15% to 30%. The composites were characterized by electrical and mechanical measurements. The dependence of the electrical properties of these composites with the metal concentration presents a percolative behaviour with a metal-insulator transition, in addition to an increment of the capacity in the neighbourhood of a critical volume concentration. This value was found to be $f_c = 0.285$, which is much higher than the theoretical value for randomly dispersed 3D composites ($f_c = 0.16$). It has been found that the incorporation of stainless steel particles to zirconia matrix, increases the toughness and decreases both the hardness and the flexural strength. The enhancement of toughness is attributed to a crack deflection mechanism as a consequence of a weak ZrO_2/stainless steel interface.

Keywords: *Zirconia/stainless steel composites, wet-processing, mechanical properties, electrical properties*

1. Introduction

Composite materials formed by an insulating matrix and metallic particles have attracted much attention due to a singular combination of properties, including mechanical[1], electrical[2] and magnetic[3]. Such properties make them excellent candidates to fabricate multifunctional devices[4]. Ceramic-metal composites are widely used in industrial applications as resistors, sensors and transducers, such as piezoresistors, and chemical sensors.

The variation of the average properties of these heterogeneous materials with the metallic content is not obvious, and in most cases they do not follow the simple rule of mixture. Moreover, the effective electrical properties for metal-ceramic composites, where there is a huge difference in conductivity between both components, are given by the percolation theory. It states that there must exist a critical concentration named *percolation threshold*[5,6] where a sharp change in the electrical properties takes place. Below this threshold the properties are similar to those of the matrix, while above that they are mainly determined by the nature of the metallic inclusions. A less known feature of the percolation theory is the divergence of the imaginary part of the conductivity, *i.e.* the real part of the dielectric constant, at the percolation threshold[7].

Brittle ceramics can be toughened by the incorporation of metallic inclusions. The toughening effect is either contributed by the plastic deformation of the metals or by crack deflection. In the present study, stainless steel is chosen as the reinforcement material for ZrO_2. The effect of the volume fraction of the metal phase on the mechanical properties (toughness, strength and hardness) of zirconia-stainless steel composite has been described.

The unique properties of metal-ceramic composites in regions close to the percolation threshold makes them adequate for a wide variety of devices applicable to detect critical changes, such as electro-mechanical sensors, wearing-sensors, etc.

The aim of the current study was to understand the processing of ZrO_2/stainless steel composites as well as their mechanical features and electrical properties. Similar studies have been carried out for other ceramic-metal sys-

*e-mail: srmello@baitaca.ipen.br

tems, such as Mullite/Mo[8] and ZrO_2/Ni[9]. In this case, stainless steel has been chosen because of its enhanced corrosion resistance, high temperature oxidation resistance and its strength. Its low cost is an attractive point facing industrial applications.

2. Experimental

2.1. Starting materials

The following commercially available powders have been used as raw materials: (1) Stainless steel powders (*Höganäs AB, Sweden*), average particle diameter $d_{50} = 21.9 \pm 0.1$ µm and chemical analysis (wt.%): Cr (14.7%), Ni (10.5%), Mo (1.75%), Mn (0.11%). (2) Tetragonal zirconia polycrystals (Y-TZP 3 mol%; *TZ-3YS, Tosoh Corp., Japan*), with an average particle size of $d_{50} = 0.6 \pm 0.1$ µm.

Size measurements of precursors were made by a light scattering procedure using a particle size analyzer *Coulter LS130*.

2.2. Sedimentation study

Different ZrO_2/stainless steel suspensions of 70 and 80 wt% solid content were prepared using distilled water as liquid media and a 1 and 3 wt% addition of an alkali-free organic polyelectrolyte as surfactant (*Dolapix PC-33*) with a relative proportion of metal of 40 vol%. The mixtures were homogenized by milling with zirconia balls in polyethylene containers at 150 r.p.m. for 24 h and then dried at 90 °C for 24 h. The sedimentation behaviour of water-based slurries was studied at room temperatures in glass test tubes for times up to 24 h.

2.3. Powder processing and sintering process

Different ZrO_2/stainless steel suspensions of 80 wt% solid content were prepared using distilled water as liquid media and a 3 wt% addition of an alkali-free organic polyelectrolyte as surfactant with a relative proportion of stainless steel ranging from 15 to 30 vol.%. The mixtures were homogenized by milling with zirconia balls in polyethylene containers at 150 r.p.m. for 24 h and then dried at 90 °C for 24 h. The resulting powders were ground in an agate mortar and subsequently passed through a 100 µm sieve. Finally, the powders were isostatically pressed at 200 MPa. The resulting cylindrical rods (≈5 mm diameter) were fired using a tubular furnace in a 90%Ar/10%H_2 atmosphere at 1350 °C for 2 h for final sintering. The heating and cooling rate was kept at 10 °C/min. For comparative purposes, a similar experimental procedure was used to obtain pure zirconia compacts.

2.4. Microstructure and density

The microstructures of fired specimens were studied on diamond polished surfaces down to 1 µm by scanning electron microscopy (*Karl-Zeiss, DSM-950 model*).

The bulk densities of all the samples were measured using the Archimedes method, with mercury as the immersion medium.

2.5. Electrical properties

Complex impedance measurements were carried out with a complex-impedance analyzer *Solartron 1260*, in frequencies ranging from 1 Hz to 1 MHz in the two points configuration. Silver electrodes were painted over both faces of each sample. The applied voltage was always lower than 0.5 V. According to the analyser specifications, all measurements were made with an experimental error less than 5%. Dielectric constant measurements were carried out at 1 kHz for insulator samples ($f = 0.15$, 0.20, 0.26 and 0.28).

2.6. Mechanical properties

Bending strength, σ_f, was determined by a three-point bending test using the resulting cylindrical rods. The tests were performed at room temperature using a universal testing machine (*Instron 4411*). The specimens were loaded to failure with a cross-head speed of 0.5 mm/min and a span of 40 mm.

The Vickers hardness, H_V, and fracture toughness, K_{IC}, were measured using a Vickers diamond indenter (*Leco 100-A*) on surfaces polished down to 1 µm, with applied loads of 490 N. The corresponding crack sizes were determined using an optical microscope (*Leica DMRM*). The fracture toughness was calculated using the formula given by Miranzo and Moya[10].

3. Results and discussion

3.1. Sedimentation and microstructure

The results obtained from the sedimentation study of the suspensions as well as the microstructural aspects are summarized in Table 1. Figure 1A shows the segregation of powders in the suspension with 70 wt.% in solid content and 1 wt.% addition of surfactant. In order to obtain a homogeneous dispersion of steel in the zirconia matrix the most convenient combination of parameters was 80 wt.% in solid content and 3 wt.% addition of surfactant. This slurry presented no segregation of powders and leaded to homogeneous fired microstructures (see Fig. 1B). Micrographs corresponding to the microstructure of samples made under these conditions with 15 vol.% and 30 vol.% metal are shown in Fig. 2. In these pictures it can be seen that metal particles are homogeneously distributed into the ceramic matrix and there is no evidence of agglomerates.

Table 1. Formulation of the suspensions used in this study and summary of experimental results.

Sample	Solids loading (wt%)	Deflocculant addition (wt%)	Sedimentation	Microstructure
70-1	70	1	Segregation	Agglomerates
70-3	70	3	Segregation	Agglomerates
80-1	80	1	Gradual segregation	F.G.M. with agglomerates
80-3	80	3	Homogeneous	Homogeneous

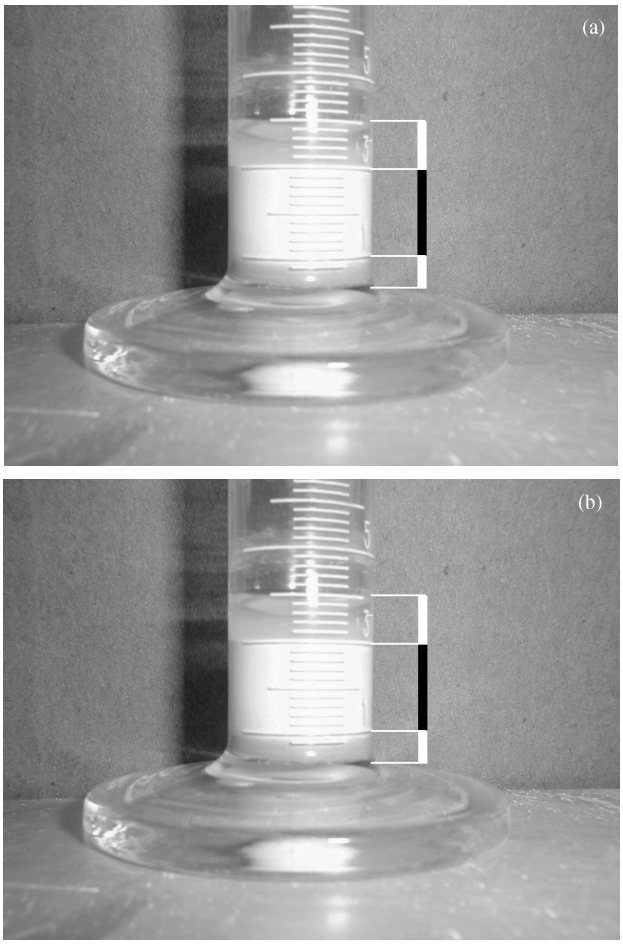

Figure 1. Sedimentation behaviour of two ZrO_2/stainless steel different suspensions: A) 70 wt.% solid loading and 1 wt.% deflocculant, B) 80 wt.% solid loading and 3 wt.% deflocculant.

The relative densities of the obtained sintered ZrO_2/stainless steel composites were found to be very close to the theoretical values (>99%th.).

3.2. Electrical measurements

We have employed capacity measurements of the insulator samples obtained from impedance spectroscopy to determine the percolation threshold of these systems instead of conductivity measurements. This is due to the fact that the chosen technique, based on the expected capacity increase at the percolation threshold, is experimentally easier to implement for highly insulating systems than

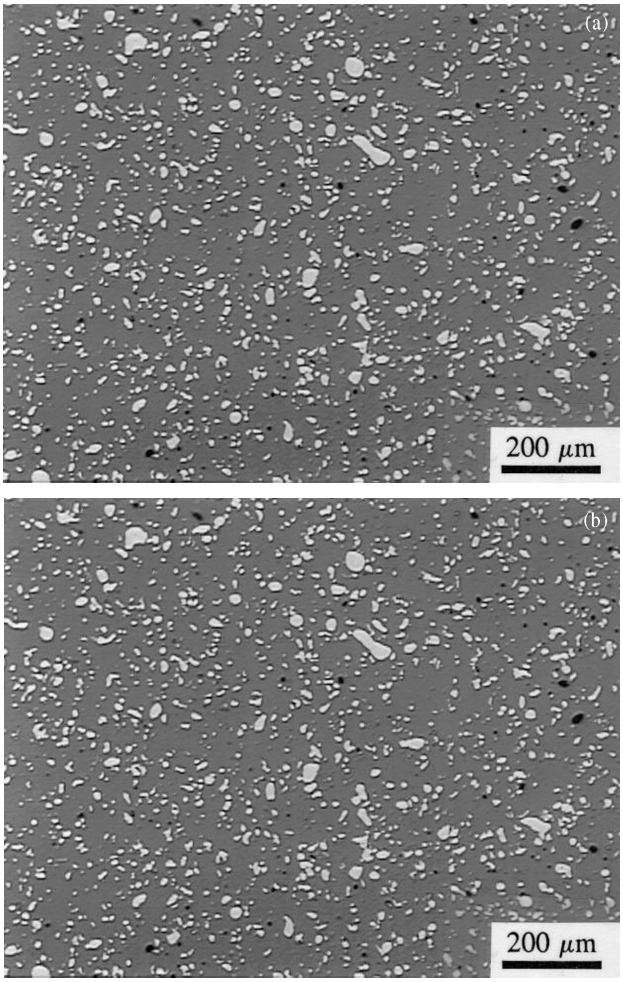

Figure 2. Optical micrographs of the polished cross section of zirconia/stainless steel composites: A) 15 vol.% metal and B) 30 vol.% metal. Lighter phase is metal and the darker phase is zirconia.

conventional DC conductance experiments. In Fig. 3 we plotted the relative dielectric constant of samples with different metal concentration. The electrical properties in the neighbourhood of the percolation threshold follow a scaling law with concentration. The general theory predicts that the behaviour of the dielectric constant is given by expression:

$$\langle \varepsilon \rangle = \varepsilon_m \left| \frac{f_c}{f_c - f} \right|^q \quad (1)$$

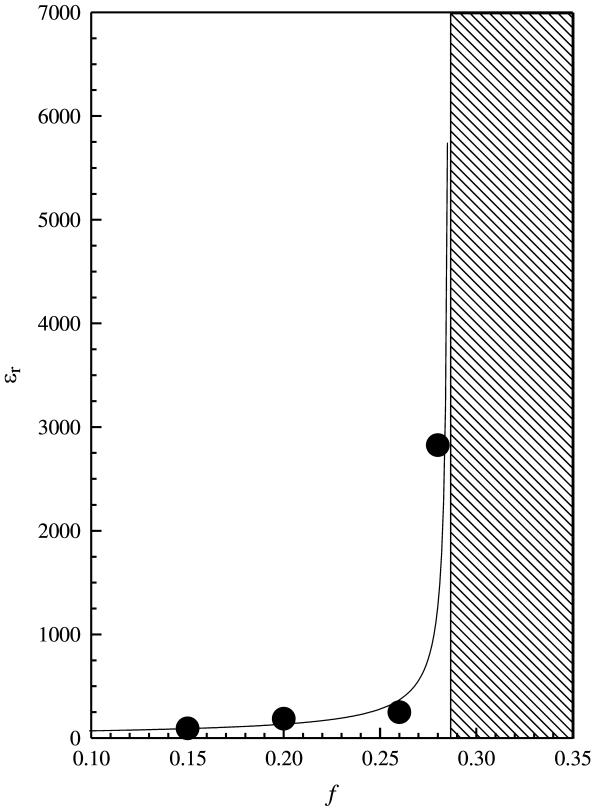

Figure 3. Relative dielectric constant (ε_r) *vs.* filling factor (f) corresponding to different monolithic ZrO_2/stainless steel composites (15, 20, 26 and 28 vol.% metal).

where ε_m is the dielectric constant of the matrix, f_c is the percolation threshold and f is the filling factor of the composite. The fit for the ZrO_2/stainless steel series to this expression gives $q = 0.84 \pm 0.06$, which is in agreement with the most common found value, $q = 0.90$. A value of percolation threshold $f_c = 0.285 \pm 0.015$ was obtained. This value is nearly twice larger than the one predicted by classical percolation theory in randomly disordered samples, probably due to an ordering process into the suspension. This phenomenon, which has been observed in ZrO_2/Ni sintered composites by a digital image treatment[9], implies the existence of a preferential distance between first neighbours in contraposition to the random distribution, in which all distances are equally probable.

3.3. Mechanical properties

The variation of bending strength, fracture toughness and Vickers hardness with the stainless steel volume fraction is shown in Fig. 4.

Since the zirconia monolithic samples have a smaller grain size, resulting in smaller intrinsic flaw dimensions, they exhibit higher strength than the ZrO_2/stainless steel composites. The *bending strength* decreasing of the ZrO_2/stainless steel composites as a function of stainless steel content can be explained considering that the average

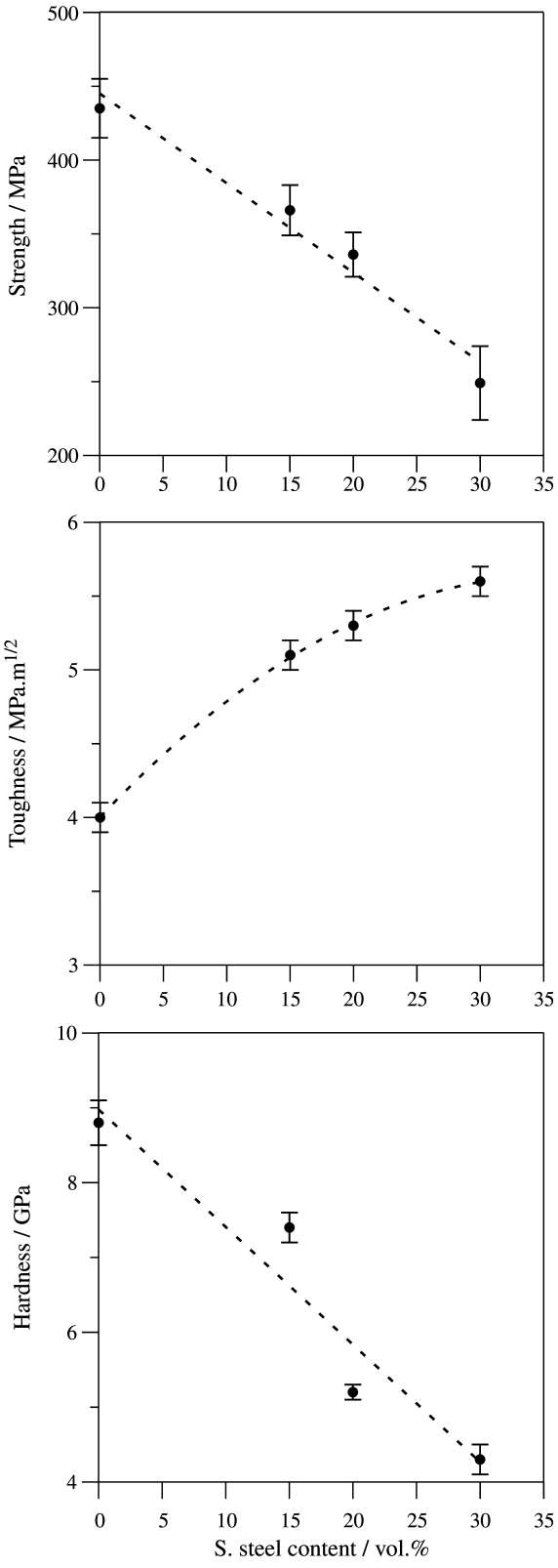

Figure 4. Mechanical properties of ZrO_2/stainless steel composites: A) Bending strength, B) fracture toughness and C) Vickers hardness. The dashed lines are guides to the eyes.

grain size of the metal particles is ≈20 μm, resulting in a higher defect size.

The *hardness* of all the zirconia/stainless steel composites is lower than that of zirconia (8.8 GPa) and it decreases as the metal content increases.

The increment in *fracture toughness* observed in the composites with higher content of metal inclusions can be assigned to the crack deflection and/or crack extension around the particles. Susceptibility to interface debonding strongly influences the quantitative effect of this micromechanism. A thermal expansion mismatch exists between the ceramic matrix and the metallic particles. Therefore, internal stresses developed during cooling of the composites are set up around the metallic inclusions. As the thermal expansion coefficient of the inclusions is bigger than that of the matrix ($\alpha_{S.\ Steel} = 18.4\ \ 10^{-6}\ °C^{-1}$ at 538 ºC and $\alpha_{ZrO2} = 11.8\ \ 10^{-6}\ °C^{-1}$ at 1000 °C), the ceramic-metal interface is subjected to a radial tensile stress. These stresses can produce deflection processes as well as an insufficiently strong interfacial bond which cause the particle debonding.

As it can be observed in Fig. 5A, the crack follows the zirconia/stainless steel interface. The crack propagates smoothly in the ceramic matrix and, on intercepting the metal particles, follows the weak ZrO_2/stainless steel interface. Figure 5B shows the fracture surface of ZrO_2/20 vol% stainless steel composite. In neither composite there was indication of plastic deformation of the metal particles during fracture.

X-ray diffraction patterns relative to the fracture surface of ZrO_2 (3Y-TZP) sintered in reducing atmosphere[11], show that there is no presence of the main peak corresponding to monoclinic pattern ($2\theta = 28.223°$). It is established that heating zirconia in reducing environments produces lost of oxygen, and, therefore, the resulting zirconia is non-stoichiometric, ZrO_{2-x}, and stability of phases may be affected[12]. Therefore, the zirconia matrix is greatly stabilized and does not afford stress-induced transformation toughening.

4. Conclusions

We have studied the processing of the ZrO_2/stainless steel system. The conditions to obtain monolithic homogeneous composites with density close to theoretical (>99%th.) at 1350 °C in reducing atmosphere have been adjusted to the optimum: 80 wt.% in solid loading and 3 wt.% in deflocculant addition.

It has been proved, by complex impedance measurements, that in wet processed ZrO_2/stainless steel composites the percolation threshold corresponds to a critical filling factor $f_c = 0.28$.

It was found that the presence of stainless steel particles decreases the strength and hardness and increases the toughness of the composites. Crack deflection due to a weak ZrO_2/stainless steel interface was found to be the main toughening mechanism in these ceramic/metal composites.

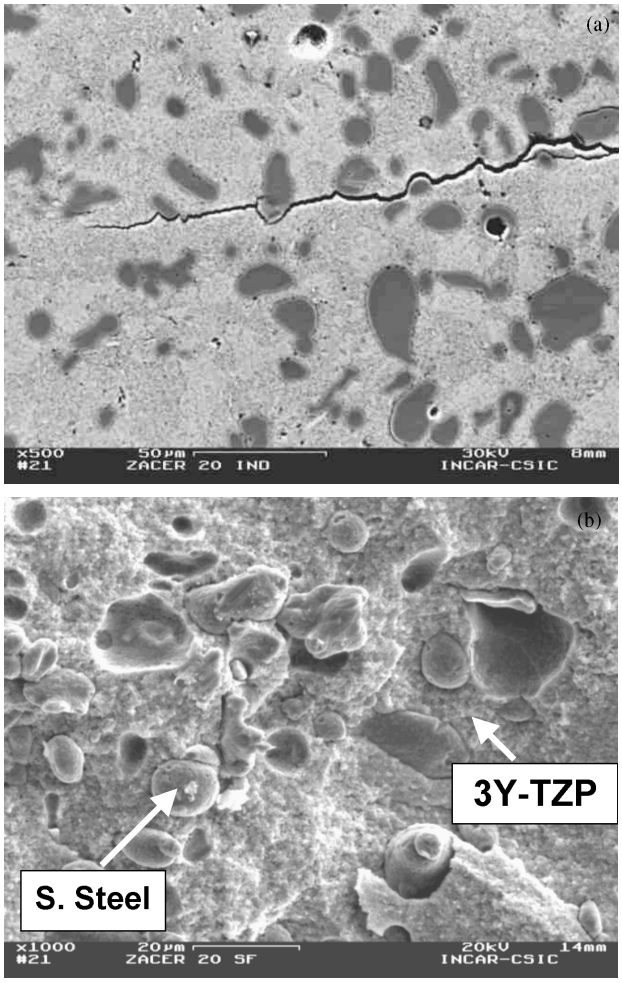

Figure 5. A) SEM micrograph illustrating the form of a crack initiated through a Vickers indentation in sample with 20 vol.% metal. Lighter phase is zirconia and the darker phase is metal. B) SEM micrograph of fracture surface of the same ZrO_2/stainless steel composite.

Acknowledgements

This work was supported by CICYT, Spain, under project number MAT97-0724, S.R.H. Mello Castanho acknowledges Mr. S. Kvist, from Höganäs for send the steel powder samples.

References

1. Krstic, D.V. *Philos. Mag. A*, v. 48, n. 5, p. 695-708, 1983.
2. Hu, W.; Guan, H.; Sun, X.; Li, S.; Fukumoto, M.; Okane, I. *J. Am. Ceram. Soc.*, v. 81, n. 8, p. 209-2212, 1998.

3. Berkowitz, A.E.; Lahut, J.A.; Van Buren, C.E. *IEEE Transactions of Magnetic Materials Magn*, v. 16, n. 2, p. 184-190, 1980.
4. Key Engineering Materials, v. 175-176. *Engineering Ceramics99: Multifunctional properties- New perspectives, Proc. of the Advanced Research Workshop on Engineering Ceramics*, v. 175-176. Sajgalík, P.; Lencés, Z., eds., Trans Tech Publications Ltd, Switzerland, 2000.
5. Kirkpatrick, S. *Rev. Modern Phys*., v. 45, n. 4, p. 574-588, 1973.
6. Stauffer, D. *Physics Reports*, v. 54, p. 3-74, 1979.
7. Efros, A.L.; Shklovskii, B.I. *Phys. Stat. Sol. (b)*, v. 76, p. 475-485, 1976.
8. Pecharromán, C.; Moya, J.S. *Adv. Mater.*, v. 12, p. 294-297, 2000.
9. Pecharromán, C.; López-Esteban, S.; Bartolomé, J.F.; Moya, J.S. *J. Amer. Ceram. Soc.* (in press).
10. Miranzo, P.; Moya, J.S. *Ceramics International*, v. 10, p. 147-152, 1984.
11. López-Esteban, S.; Bartolomé, J.F.; Moya, J.S.; Tanimoto, T. *J. Mater. Res.*, (in press).
12. Hanson, W.B.; Ironside, K.I.; Fernie, J.A. *Acta Mater.*, v. 48, p. 4673-4676, 2000.

FAPESP helped in meeting the publication costs of this article